uc3m | Universidad Carlos III de Madrid

e-Archivo

This is a postprint version of the following published document:

Soria-Verdugo, A. … et al. (2014) Evaluating the accuracy of the Distributed Activation Energy Model for biomass devolatilization curves obtained at high heating rates, *Energy Conversion and Management*, v. 86, p.: 1045-1049.

DOI: https://doi.org/10.1016/j.enconman.2014.06.074

© 2014 Elsevier Ltd. All rights reserved.

This work is licensed under a Creative Commons AttributionNonCommercialNoDerivatives 4.0 International License

Evaluating the accuracy of the Distributed Activation Energy Model for biomass devolatilization curves obtained at high heating rates

A. Soria-Verdugo*, L.M. Garcia-Gutierrez, L. Blanco-Cano, N. Garcia-Hernando, U. Ruiz-Rivas

Carlos III University of Madrid (Spain)

Energy Systems Engineering Group, Thermal and Fluids Engineering Department

Avda. de la Universidad 30, 28911, Leganés (Madrid, Spain)

* corresponding author: asoria@ing.uc3m.es Tel: +34916248884. Fax: +34916249430.

ABSTRACT

The characteristic parameters of devolatilization, the activation energy and the frequency factor, can be obtained following different experimental approaches. In the Distributed Activation Energy Model (DAEM), these parameters are derived from several TGA curves that are typically obtained for constant, low heating rate experiments. Then, the results are used to model high heating rate processes typical of industrial combustors. In this work, a wide range of heating rates were employed to obtain different TGA curves of the biomass pyrolysis, in order to analyse the validity of DAEM when extrapolating the kinetic parameters obtained for low heating rate curves used in the laboratory to higher heating rates present in industrial applications. The TGA curves of the biomass pyrolysis employed in DAEM were varied from low heating rates (around 10 K/min, values typically found in the literature

on DAEM), to high heating rates (up to 200 K/min). The differences in the activation energy and the frequency factor obtained for different heating rates, were evaluated and the validity of the model was discussed. The results show differences between the activation energy and the frequency factor obtained using low and high heating rates during the TGA tests. Therefore, if an accurate approximation is required when extrapolating the data to high heating rates, the tests should be carried out at high heating rates.

KEYWORDS

Distributed Activation Energy Model, devolatilization, pyrolysis, biomass conversion, activation energy, heating rate.

NOMENCLATURE

a	Heating rate [K/s].
E_a	Activation energy for a determined devolatilization rate [J/mol].
k_0	Frequency factor for a determined devolatilization rate [s^{-1}].
R	Universal constant [J/mol·K].
R^2	Determination coefficient of the linear fitting [-].
T	Temperature [K].
V	Volatile mass loss [%].
V^*	Volatile content [%].
V/V^*	Devolatilization rate [%].

ε Relative error [%].

1. Introduction

Biomass pyrolysis takes place during most of the processes related to biomass thermochemical conversion, such as production of liquid biofuels [1], synthesis gas [2], chemicals [3], or charcoal [4], becoming a key factor in most applications. The characteristic parameters that control the kinetics of biomass devolatilization are the activation energy (E_a) and the frequency factor (k_0). Several models are available in literature to describe biomass pyrolysis [5], [6], [7], and between them the Distributed Activation Energy Model (DAEM) proposed by Vand [8] has been widely used due to its simplicity and accuracy. Miura and Maki [9] simplified the model to estimate the activation energy and the corresponding frequency factor from three TGA curves obtained for different heating rates. This simplification has been used to describe the kinetics of pyrolysis for different types of biomass [10], [11], [12], [13], [14], coal [15], [16], sewage sludge [17], [18], and waste [19], [20], [21].

The heating rates employed using DAEM are usually low, in the range of 3 to 30 K/min, due to the higher accuracy of TGA at reduced heating rates. Miura and Maki [9] proposed the use of heating rates of 5, 10 and 20 K/min, but Sonobe et al. [10] employed even lower heating rates 2, 4 and 10 K/min. Shen et al. [11] employed heating rates between 5 and 40 K/min and Soria-Verdugo et al. [18] used heating rates of 10, 15, 20 K/min. Despite of the variety of heating rates found in the literature most of the authors used heating rates below 50 K/min. As an exception, Li et al. [15] used heating rates of 20, 35, 50, 75 and 100 K/min during the devolatilization of coals and biomass in a thermogravimetric analyzer, nevertheless there is no available data for heating rates beyond 100 K/min.

In this work, a wider range of heating rates (3, 5, 10, 15, 20, 30, 50, 80, 100, 150 and 200 K/min) were employed to obtain different TGA curves, in order to analyse the validity of the simplified Distributed Activation Energy Model, when extrapolating the kinetic parameters obtained for low heating rate curves to higher heating rates. The simplified DAEM process described by Miura and Maki [9] to obtain the pyrolysis parameters was analyzed for the different heating rates, therefore the three TGA curves employed were varied from very low heating rates (3, 5 and 10 K/min) to higher heating rates (100, 150 and 200 K/min). The differences in the activation energy and the frequency factor were evaluated and the validity of the model was discussed.

2. Experimental procedure

The biomass employed during the tests was obtained from commercial pine pellets. The biomass characterization results of a proximate and ultimate analysis are presented in Table 1. The proximate analysis was performed in a TGA Q500 TA Instruments, while the ultimate analysis was carried out in a LECO TruSpec CHN and TruSpec S elemental analyzer. The moisture of the sample was obtained after an isothermal process at 105ºC under an inert atmosphere in the TGA, whereas the volatile content was determined heating the sample up to 900ºC under an inert atmosphere, and maintaining the temperature until no difference in the mass of the sample was observed. The ash content was measured as the constant mass of the sample remaining after an isothermal process at 550ºC under and oxidant atmosphere. Finally, the fixed carbon of the sample was obtained by difference.

Proximate analysis[a]	
Moisture [%]	3.3
Volatiles [%]	76.3
Fixed carbon[b] [%]	17

Ash [%]	3.4
Ultimate analysis[a]	
C [%]	46.13
H [%]	6.51
N [%]	0.82
S [%]	0.07
O[b] [%]	46.47

Table 1. Thermochemical characterization of the biomass employed ([a] wet basis, [b] obtained by difference).

The devolatilization tests were carried out in the same thermogravimetric analyzer TGA Q500 TA Instruments employed to obtain the biomass proximate analysis. During the experiments, the TGA furnace was flushed with 60 ml/min of nitrogen to maintain an inert atmosphere. The mass of the samples were 10±0.5 mg and they were sieved under 100 μm to avoid heat transfer effects, according to Di Blasi et al. [22]. A blank experiment was also run for any case studied to avoid buoyancy effects [11], [12]. Each test was repeated five times to guarantee repeatability, obtaining differences always lower than 3%.

Once the sample was introduced in the TGA, it was heated up to 105ºC from room temperature, and an isothermal process was maintained during 20 minutes to eliminate all the moisture content. Then, the devolatilization process begins, and the temperature increases with a constant heating rate *a* until 600ºC. Fig. 1 shows the weight loss and the temperature versus time for the TGA analysis using heating rates *a* of 20 and 200 K/min during the devolatilization process. The drying process is the same for both tests so the weight loss curves collapsed during the first part of the analysis, nevertheless the different heating rates employed in the devolatilization process produced significant differences on the sample weight loss curves when the pyrolysis occurred. Depending on the heating rate used during the devolatilization

process, the time needed for the test can be very different, from 68 minutes for the heating rate of 20 K/min to just 45 minutes when using 200 K/min, nonetheless the weight percentage loss at the end of the devolatilization is independent of the heating rate employed. During the experiments several heating rates were employed during the devolatilization process, in a wide range: *3, 5, 10, 15, 20, 30, 50, 80, 100, 150*, and *200 K/min*. In the case of a heating rate of 3 K/min, 210 minutes were needed to perform the test.

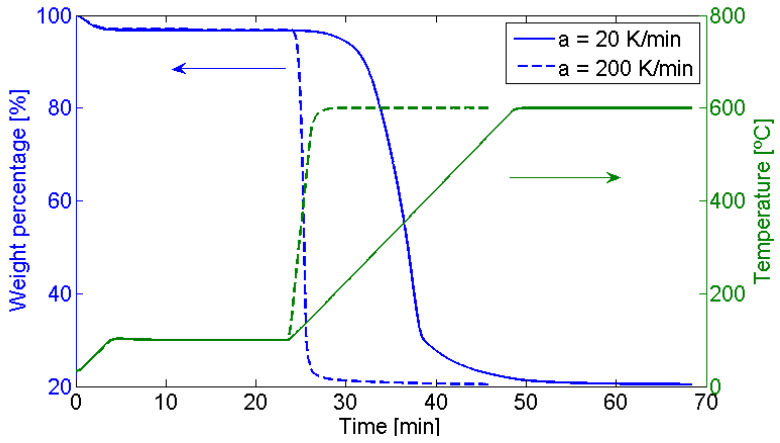

Figure 1: Example of a thermogravimetric analysis (*a = 20 K/min* and *200 K/min*)

Finally, since this work is not focused in the drying process but in the devolatilization process, the range of devolatilization can be obtained from the TGA curve (Fig. 1), defining a devolatilization rate of 0% at the end of the isothermal process at 105ºC, and 100% when the temperature is 550ºC, ensuring a constant heating rate, *a*, for the whole devolatilization process. Fig. 2 shows the devolatilization rate as a function of temperature for the same heating rates depicted in Fig. 1. It can be observed that most of the devolatilization process occurs between 300ºC and 400ºC, obtaining a sharp devolatilization rate typical of cellulose.

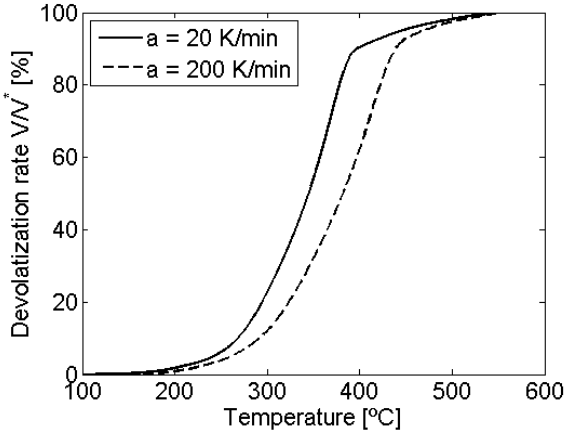

127

128 Figure 2: Devolatilization rate against temperature (*a = 20 K/min, 200 K/min*)

129 **3. Simplified DAEM model**

130 The Distributed Activation Energy Model has been proved to be an accurate method
131 to describe the pyrolysis kinetics of biomass, obtaining a good agreement with the
132 experimental data [10], [23], [24], and [25], when operating at low heating rates. The
133 model assumes the existence of an infinite number of irreversible first order reactions
134 occurring sequentially, with different associated activation energies, E_a. The
135 devolatilization process can be described in the integral form by Eq. 1:

136 $$1-\frac{V}{V^*}=\int_0^{\infty}\exp\left(-k_0\int_0^t e^{-E/RT}dt\right)f(E)dE \qquad (1)$$

137 where V/V^* is the devolatilization rate, R the universal constant, T the temperature for
138 each devolatilization and $f(E)$ the distribution function of the activation energy. This
139 equation was simplified to Eq. 2 by Miura et al. [26]

140 $$V/V^* \cong 1-\int_{E_a}^{\infty} f(E_a)dE_a=\int_0^{E_a} f(E_a)dE_a \qquad (2)$$

141 The Arrhenius equation of the simplified DAEM model is:

$$\ln\left(\frac{a}{T^2}\right) = \ln\left(\frac{k_0 R}{E_a}\right) + 0.6075 - \frac{E_a}{R}\frac{1}{T} \quad (3)$$

The values of the activation energy, E_a, and the corresponding frequency factor, k_0, present in Eq. 3 can be obtained from three different thermogravimetric curves obtained with different heating rates. Miura and Maki [9] proposed a procedure following the next steps:

a) Measure and plot the devolatilization rate, V/V^*, as a function of the temperature, T, for three different heating rates, a.
b) Plot $\ln(a/T^2)$ versus $1/T$ for the three different heating rates at each devolatilization rate (Arrhenius plot).
c) For each V/V^* in the Arrhenius plot, linearize the data of the different heating rates and obtain E_a and k_0 from the slope and the intercept respectively.

4. Results and discussion

Thermogravimetric tests were carried out for heating rates of 3, 5, 10, 15, 20, 30, 50, 80, 100, 150, and 200 K/min, obtaining the devolatilization rates plotted in Fig. 3 for each heating rate. The devolatilization takes place at higher temperatures when increasing the heating rate, a result previously reported in the literature that can be atributed to non-isothermal pyrolysis processes [27], [28].

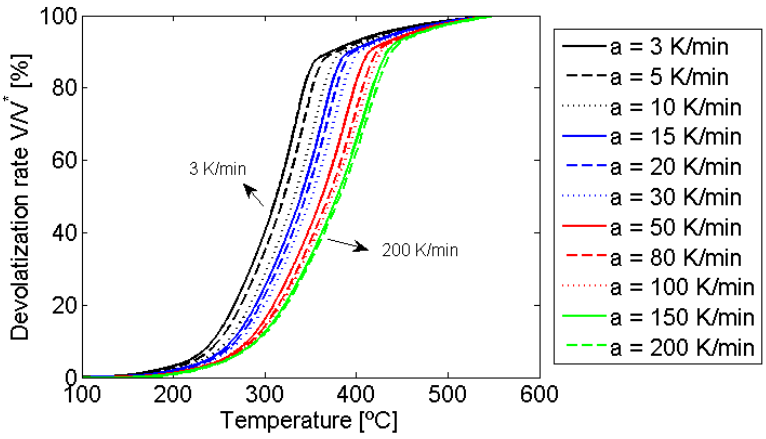

159

160 Figure 3: Devolatilization rate versus temperature for each heating rate.

161 Following the procedure proposed by Miura and Maki [9], the temperature at which
162 each devolatilization rate occurs can be obtained from Fig. 3, for each heating rate.
163 With these temperatures, an Arrhenius plot can be built, plotting $\ln(a/T^2)$ versus $1/T$,
164 as shown in Fig. 4 for each devolatilization rate, with variations of 5%.

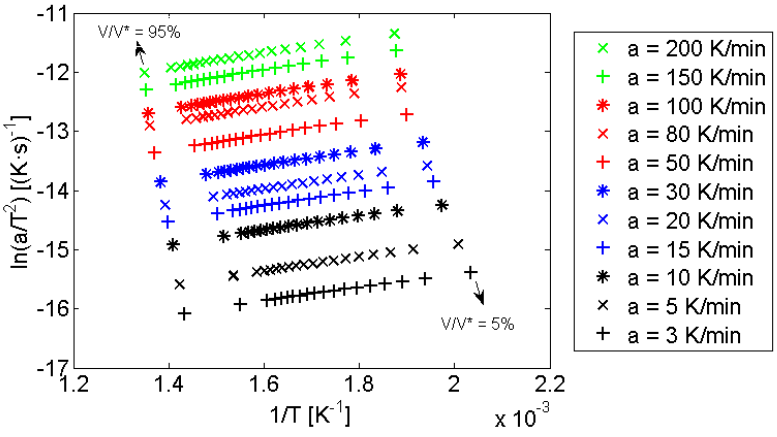

165

166 Figure 4: Arrhenius plot for each devolatilization rate.

167 The next step in the procedure described by Miura and Maki [9] is the linearization of
168 the results shown in the Arrhenius plot for each devolatilization rate. Analising Fig. 4
169 for low devolatilization rates ($V/V^* = 5\%$), it can be observed that there is a change in
170 the slope of the linearization curve for heating rates over 50 K/min. For high

devolatilization rates this is not so evident. In order to quantify the goodness of a linear fitting of the results considering all the heating rates, the determination coeficient, R^2, of the linear fitting is shown in Fig. 5, as a function of the devolatilization rate. The determination coeficient is found to be lower at low devolatilization rates informing of a poor linearity of the data in this zone, confirming the idea that there is a change in slope for low devolatilization rates obtained from the visual inspection of Fig. 4.

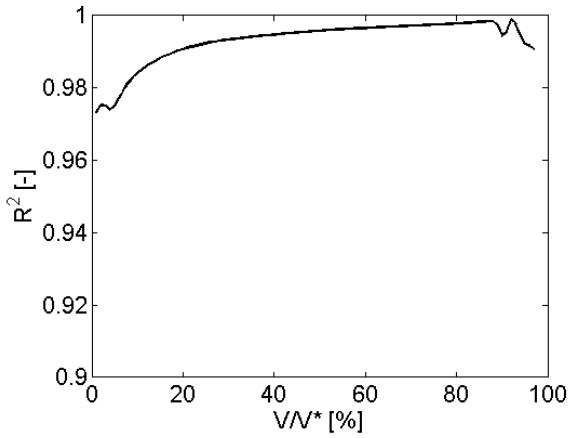

Figure 5: Determination coefficient of the linear fitting for all the heating rates as a function of the devolatilization rate.

The linearization of the results shown in the Arrhenius plot (Fig. 4) was carried out regrouping the data for three different heating rates as suggested by Miura and Maki [9]. The experimental data allows to linearize the results for very low heating rates (*a = 3, 5, 10 K/min*), low heating rates (*a = 15, 20, 30 K/min*), medium heating rates (*a = 50, 80, 100 K/min*) and high heating rates (*a = 100, 150, 200 K/min*), in order to quantify the variation of slope stated above. The linearization of the results for each group of heating rates provides an slope, *m*, and an intercept, *n*, from which the activation energy, E_a, and the frequency factor, k_0, can be easily obtained in view of Eq. 3, obtaining Eq. 4 and 5.

$$E_a = -m \cdot R \tag{4}$$

$$k_0 = -m \cdot e^{n-0.6075} \tag{5}$$

The values of the activation energy and the frequency factor are presented in Fig. 6 a) and b) respectively, as a function of the devolatilization rate for very low, low, medium and high heating rates. There is a clear difference in both the activation energy and the frequency factor when linearizing the results obtained for low and high heating rates. These parameters increase when higher heating rates are employed, confirming the existence of a higher slope in the linearization of the high heating rate TGA curves (*a = 100, 150, 200 K/min*). The difference is larger at low devolatilization rates, as established in Fig. 5.

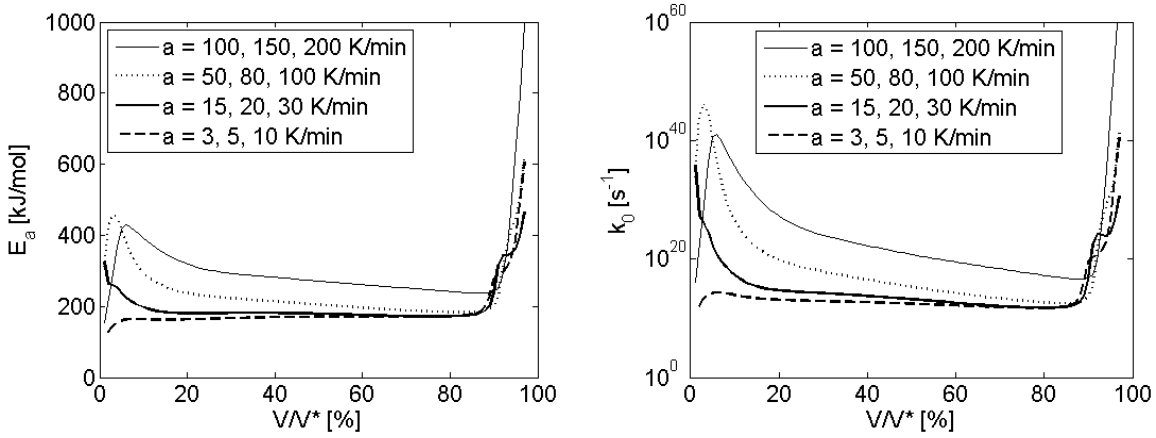

Figure 6: a) Activation energy and b) frequency factor for each devolatilization rate.

The difference in activation energy obtained between each group of heating rates and the higher one can be analyzed by means of a relative error, ε, defined in Eq. 6.

$$\varepsilon = 100 \cdot \frac{E_{a\_i,j,k} - E_{a\_100,150,200}}{E_{a\_100,150,200}} \tag{6}$$

205 The results of the relative error in activation energy can be observed in Fig. 7. A
206 relative error around 20% for the medium heating rates (*a = 50, 80, 100 K/min*) and
207 around 40% for low (*a = 15, 20, 30 K/min*) and very low heating rates (*a = 3, 5, 10*
208 *K/min*) is found for devolatilization rates between 20 and 80%, that is, for most of the
209 devolatilization process. Therefore, an error around 40% is made when determining
210 the activation energy with low heating rate TGA curves typically found in the literature
211 and extrapolating the results to high heating rates.

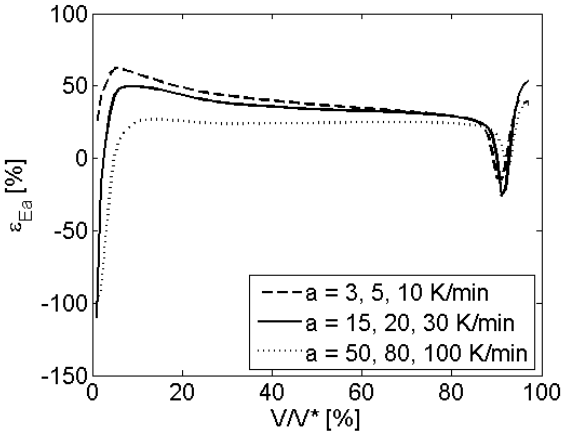

212

213 Figure 7: Relative error of the activation energy obtained from low and high heating
214 rates.

215 Finally, with the activation energy and the pre-exponential factor, the devolatilization
216 curve for a heating rate of 200 K/min can be recuperated and the differences
217 between the experimental curve obtained from the TGA and the curve recuperated
218 using DAEM can be evaluated. The recuperation could be carried out by solving the
219 temperature in Eq. 9 or linearizing the Arrhenius plot for each heating rate, as
220 described in [19], with negligible differences. The differences between the TGA curve
221 obtained for a heating rate of 200 K/min and the curve recuperated using the
222 Distributed Activation Energy Model with low (*a = 15, 20, 30 K/min*) and high heating

rates (*a = 100, 150, 200 K/min*) were analyzed by means of the devolatilization rate error and the temperature error described in Eq. 7 and 8 respectively.

$$\varepsilon_{V/V^*} = 100 \cdot \frac{V/V^*_{DAEM} - V/V^*_{TGA}}{V/V^*_{TGA}} \quad (7)$$

$$\varepsilon_T = 100 \cdot \frac{T_{DAEM} - T_{TGA}}{T_{TGA}} \quad (8)$$

The error obtained for the devolatilization rate is plotted in Fig. 8 a). It can be observed that the DAEM recuperated curve coincided with the experimental curve when using the high heating rates (*a = 100, 150, 200 K/min*), obtaing and error close to zero. Nevertheless, when recuperating the curve with the activation energy and pre-exponential factor obtained for low heating rates (*a = 15, 20, 30 K/min*) the error in devolatilization rate is not negligible. In this case a higher error is obtained for low temperatures where the devolatilization rate is low, but for temperatures between 300ºC and 400ºC, where most of the devolatilization process occurs, the devolatilization error is between 5 and 10%. In the case of the temperature error, show in Fig. 8 b), the value of the error is around 1% for devolatilization rates between 20 and 80%. The higher error obtained for the devolatilization rate, in comparison to that of the temperature, is motivated by the high slope shown in the devolatilization rate curve (Fig. 2) for this type of biomass.

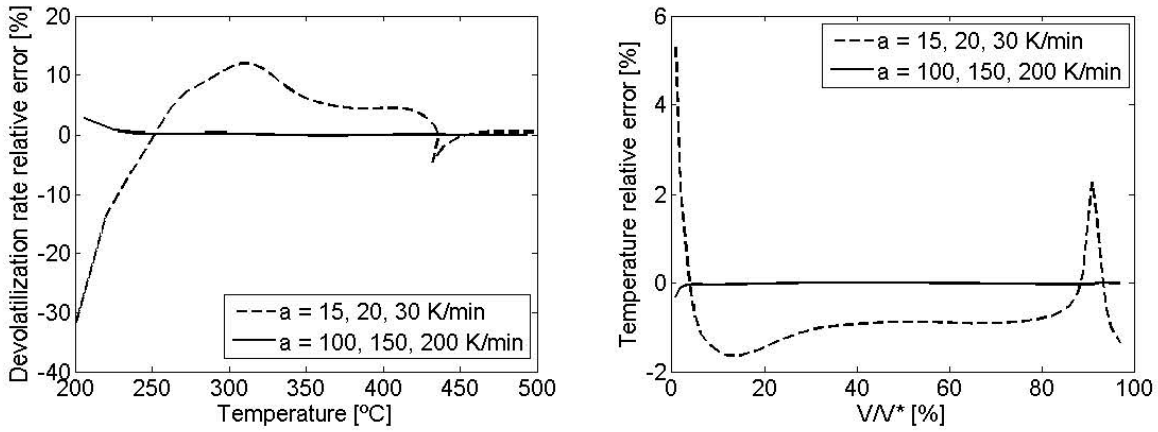

Figure 8: Error between the TGA curve for a heating rate of *200 K/min* and the curve recuperated using DAEM, a) Devolatilization rate error b) Temperature error.

This result show a certain weakness of the standard process of obtaining the devolatilization parameters, E_a and k_0, at low heating rates, as defined by Miura and Maki [9]. Even though the error obtained when extrapolating the activation energy obtained for low heating rates to higher rates can be as high as 50%, the final error obtained in the devolatilization curve is around 10% for V/V^* and just 1% for T. This error should be considered for and accurate description of the devolatilization process.

5. Conclusions

The Distributed Activation Energy Model (DAEM) was applied to study pine pellets devolatilization. The model is based on TGA curves obtained for several heating rates, from low heating rates usually found in literature (*3, 5, 10, 15, 20, 30, 50 K/min*) to higher heating rates rarely reported (*80, 100, 150, 200 K/min*).

The Miura and Maki procedure was employed to obtain the activation energy and the frequency factor for each devolatilization rate. The procedure was repeated for very low heating rate curves (*3, 5, 10 K/min*), low heating rate curves (*15, 20, 30 K/min*),

medium values (*50, 80, 100 K/min*) and high heating rates (*100, 150, 200 K/min*) to analyze the possible differences obtained. Such differences were quantified obtaining a relative error for the activation energy around 40% when extrapolating the results of low heating rates to higher ones. Nonetheless, when comparing the experimental devolatilization curve for a heating rate of *200 K/min* with the curve obtained applying DAEM to low heating rates, the error in the devolatilization rate is under 10% and the error in temperature is just 1%.

Therefore, care should be taken when employing DAEM from low heating rate TGA curves and extrapolating the results to high heating rates typical of industrial combustors.

Acknowledgments

The authors would like to express appreciation for the financial support from Projects DPI2009-10518 (MICINN) and CARDENER-CM (S2009ENE-1660).

REFERENCES

[1] A.E., Pütün, B., Burcu Uzun, E., Apaydin, E., Pütün, Bio-oil from olive oil industry wastes: Pyrolysis of olive residue under different conditions. Fuel Process. Technol. 2005; 87: 25-32.

[2] S., Kaewluan, S., Pipatmanomai, Potential of synthesis gas production from rubber wood chip gasification in a bubbling fluidised bed gasifier. Energy Convers. Manag. 2011; 52: 75-84.

[3] F., Orecchini, E., Bocci, Biomass to hydrogen for the realization of closed cycles of energy resources. Energy. 2007; 32: 1006-1011.

[4] M.J., Prins, K.J., Ptasinski, F.J.G., Janssen, Torrefaction of wood: Part 1. Weight loss kinetics. J. Anal. Appl. Pyrolysis. 2006; 77: 28-34.

[5] A.W., Coats, J.P., Redfern, Kinetic parameters from thermogravimetric data. Nature. 1964; 201: 68-69.

[6] S.K., Ubhayacar, D.B., Stickler, C.W., Von Rosenberg, R.E., Gannon, Rapid devolatilization of pulverized coal in hot combustion gases. In: 16th Symp. Combust. 1976.

[7] Z., Li, W., Zhao, B., Meng, C., Liu, Q., Zhu, G., Zhao, Kinetic study of corn straw pyrolysis: Comparison of two different three-pseudocomponent models. Bioresour. Technol. 2008; 99: 7616-7622.

[8] V., Vand, A theory of the irreversible electrical resistance changes of metallic films evaporated in vacuum. Proc. Phys. Societ. 1942; 55: 222-246.

[9] K., Miura, T., Maki, A simple method for estimating f(E) and K_0(E) in the distributed activation energy model. Energy Fuels. 1998; 12: 864-869.

[10] T., Sonobe, N., Worasuwannarak, Kinetic analyses of biomass pyrolysis using the distributed activation energy model. Fuel. 2008; 87: 414-421.

[11] D.K., Shen, S., Gu, B., Jin, M.X., Fang, Thermal degradation mechanisms of wood under inert and oxidative environments using DAEM methods. Bioresour. Technol. 2011; 102: 2047-2052.

[12] S., Hu, A., Jess, M., Xu, Kinetic study of Chinese biomass slow pyrolysis: Comparison of different kinetic models. Fuel. 2007; 86: 2778-2788.

[13] J., Cai, R., Liu, New distributed activation energy model: Numerical solution and application to pyrolysis kinetics of some types of biomass. Bioresour. Technol. 2008; 99: 2795-2799.

[14] K., Kirtania, S., Bhattacharya, Application of the distributed activation energy model to the kinetic study os pyrolysis of the fresh water algae Chlorococcum humicola. Bioresour. Technol. 2012; 107: 476-481.

[15] Z., Li, C., Liu, Z., Chen, J., Qian, W., Zhao, Q., Zhu, Analysis of coals and biomass pyrolysis using the distributed activation energy model. Bioresour. Technol. 2009; 100: 948-952.

[16] M., Günes, S.K., Günes, Distributed activation energy model parameters of some Turkish coals. Energy Sources Part A-Recovery Utilization and Environmental Effects. 2008; 30: 1460-1472.

[17] S.A., Scott, J.S., Dennis, J.F., Davidson, A.N., Hayhurst, Thermogravimetric measurements of the kinetics of pyrolysis of dried sewage sludge. Fuel. 2006; 85: 1248-1253.

[18] A., Soria-Verdugo, N., Garcia-Hernando, L.M., Garcia-Gutierrez, U., Ruiz-Rivas, Analysis of biomass and sewage sludge devolatilization using the distributed activation energy model. Energy Conv. and Manag. 2013; 65: 239-244.

[19] J.H., Yan, H.M., Zhu, X.G., Jiang, Y., Chi, K.F., Cen, Analysis of volatile species kinetics during typical medical waste materials pyrolysis using a distributed activation energy model. J. Hazard. Mater. 2009; 162: 646:651.

322 [20] L., Li, N., Zhao, X., Fu, M., Shao, S., Qin, Thermogravimetric and kinetic analysis of
323 Spirulina wastes under nitrogen and air atmospheres. Bioresour. Technol. 2013; 140:
324 152-157.

325 [21] L., Fiori, M., Valbusa, D., Lorenzi, L., Fambri, Modeling of the devolatilization
326 kinetics during pyrolysis of grape residues. Bioresour. Technol. 2012; 103: 389-397.

327 [22] C., Di Blasi, C., Branca, A., Santoro, E., Gonzalez Hernandez, Pyrolytic behavior
328 and products of some wood varieties. Combust. Flame. 2001;124: 165-177.

329 [23] J., Cai, R. Liu, Weibull mixture model for modeling nonisothermal kinetics thermally
330 simulated solid-state reactions: application to simulated and real kinetic conversion
331 data. J. Phys. Chem. 2007; 111: 10681-10686.

332 [24] J., Cai, L., Ji, Pattern search method for determination of DAEM kinetic parameters
333 from nonisothermal TGA data of biomass. J. Math. Chem. 2007; 42: 547-553.

334 [25] T., Mani, P., Murugan, N., Mahinpey, Determination of distributed activation energy
335 kinetic parameters using annealing optimization method for nonisothermal pyrolysis of
336 lignin. Ind. Eng. Chem. Res. 2009; 48: 1464-1467.

337 [26]

338 [27] S., Munir, S.S., Daood, W., Nimmo, A.M., Cunliffe, B.M., Gibbs, Thermal analysis
339 and devolatilization kinetics of cotton stalk, sugar cane bagasse and shea meal under
340 nitrogen and air atmospheres. Bioresour. Technol. 2009; 100: 1413-1418.

341 [28] Y., Tonbul, A., Saydut, K., Yurdako, C., Hamamci, A kinetic investigation on the
342 pyrolysis of Seguruk asphaltite. J. Therm. Anal. Calorim. 2009; 95: 197-202.